

# Finite-Aperture Fluid Antenna Array Design: Analysis and Algorithm

Zhentian Zhang, *Graduate Student Member, IEEE*, Kai-Kit Wong, *Fellow, IEEE*, Hao Jiang, *Senior Member, IEEE*, Farshad Rostami Ghadi, *Member, IEEE*, Hyundong Shin, *Fellow, IEEE*, and Yangyang Zhang

**Abstract**—Finite-aperture constraints render array design non-trivial and can undermine the effectiveness of classical sparse geometries. This letter provides universal guidance for fluid antenna array (FAA) design under a fixed aperture. We derive a closed-form Cramér–Rao bound (CRB) that unifies conventional and reconfigurable arrays by explicitly linking the Fisher information to the geometric variance of port locations. We further obtain a closed-form probability density function of the minimum spacing under random FAA placement, which yields a principled lower bound for the minimum-spacing constraint. Building upon these analytical insights, we then propose a gradient-based algorithm to optimize continuous port locations. Utilizing a simple gradient update design, the optimized FAA can achieve about a 30% CRB reduction and a 42.5% reduction in mean-squared error.

**Index Terms**—Fluid antenna system (FAS), finite-aperture array, Cramér–Rao Bound (CRB), mean square error (MSE).

## I. INTRODUCTION

**L**INEAR array design [1] is pivotal for sensing estimation such as angle-of-arrival (AoA). Port placement strongly greatly affects estimation precision and side-lobe behavior. *If the antenna aperture budget is flexible*, various array structures [2], e.g., nested arrays, coprime arrays, and minimum redundancy arrays (MRA) [3], can significantly outperform the half-wavelength uniform linear array (ULA). However, array design becomes more challenging under *finite-aperture* constraints, in which existing methods are not necessarily effective when the aperture is limited, and a flexible architecture is preferred.

Recently, the fluid antenna system (FAS) was proposed [4] and it is a hardware-agnostic system concept that regards the antenna as a reconfigurable physical-layer resource to broaden system design with new degree of freedom (DoF) [5], [6], [7], [8]. FAS has been employed to utilize antenna reconfiguration for flexible beamforming [9], sensing [10], [11] and multiple access [12]. Despite the potential, fluid antenna array (FAA) design under finite-aperture constraints is not explored. While [11] provided an upper bound for finite-aperture AoA sensing, fundamental limits and design rules for FAA are missing.

In this work, we provide universal guidance for FAA design under finite-aperture budgets by clarifying fundamental geometric limits under fixed array length, and we further propose

Z. Zhang and H. Jiang are with the National Mobile Communications Research Laboratory, Southeast University, Nanjing, 210096, China and H. Jiang is also with the School of Artificial Intelligence, Nanjing University of Information Science and Technology, Nanjing 210044, China. (e-mail: zhentianzhangzzt@gmail.com, jianghao@nuist.edu.cn).

K. K. Wong and F. R. Ghadi are with the Department of Electronic and Electrical Engineering, University College London, Torrington Place, WC1E 7JE, United Kingdom (e-mails: {kai-kit.wong, f.rostamighadi}@ucl.ac.uk). K. K. Wong is also affiliated with the Department of Electronic Engineering, Kyung Hee University, Yongin-si, Gyeonggi-do 17104, Republic of Korea.

H. Shin is with the Department of Electronics and Information Convergence Engineering, Kyung Hee University, Yongin-si, Gyeonggi-do 17104, Republic of Korea (e-mail: hshin@khu.ac.kr).

Y. Zhang is with Kuang-Chi Science Limited, Hong Kong SAR, China (e-mail: yangyang.zhang@kuang-chi.com).

Corresponding authors: K.-K. Wong

a practical FAA design algorithm to validate the analysis. The contributions are summarized as follows:

- First, we derive a closed-form Cramér–Rao Bound (CRB) that captures different geometries under finite-aperture constraints, unifying reconfigurable array analyses.
- We characterize the minimum port spacing from a distributional perspective by deriving a closed-form probability density function (PDF), matching Monte-Carlo results.
- Finally, we propose a gradient-based algorithm based on the derived insights, validating the analytical results.

**Notations**—Scalars, vectors, and matrices are denoted by  $a$ ,  $\mathbf{a}$ , and  $\mathbf{A}$ , respectively.  $(\cdot)^T$ ,  $(\cdot)^H$ ,  $(\cdot)^*$ ,  $\|\cdot\|_2$ ,  $\otimes$ , and  $\text{vec}(\cdot)$  are transpose, Hermitian transpose, complex conjugate,  $\ell_2$ -norm, Kronecker product, and vectorization.  $\mathbb{E}[\cdot]$  is expectation.

## II. SYSTEM MODEL

### A. Finite Aperture Configuration

Consider a linear FAA at the base station (BS) with  $M$  active ports whose locations are to be optimized. The physical aperture normalized by the wavelength  $\lambda$  is  $W_{\max} = (M - 1)/2$ , which matches a ULA of  $M$  elements spaced by  $\lambda/2$ . Exploiting the flexibility of FAA, the port locations are modeled as continuous variables collected in  $\mathbf{p} = [p_1, \dots, p_M]^T \in \mathbb{R}^M$ , where  $p_m$  denotes the normalized position of the  $m$ -th port. To maximize the effective aperture, the *first* and *last* ports are fixed at the aperture boundaries, i.e.,  $p_1 = 0$ , and  $p_M = W_{\max}$ . Simultaneously, the intermediate ports are constrained within the same aperture, i.e.,  $0 < p_2 < \dots < p_{M-1} < W_{\max}$ . Additionally, to avoid the overlapping of multiple ports, a minimum inter-port spacing  $d_{\min}$  is prescribed as

$$p_m - p_{m-1} \geq d_{\min}, \quad m = 2, \dots, M. \quad (1)$$

### B. Signal Model

Without loss of generality, we consider line-of-sight transmission. The steering vector  $\mathbf{a}(\theta, \mathbf{p}) \in \mathbb{C}^M$  of AoA  $\theta$  under port placement  $\mathbf{p}$  can be expressed as

$$\mathbf{a}(\theta, \mathbf{p}) = [e^{-j2\pi p_1 \cos \theta}, \dots, e^{-j2\pi p_M \cos \theta}]^T. \quad (2)$$

The received signal vector  $\mathbf{y}(t) \in \mathbb{C}^M$  in far-field transmission at the  $t$ -th time snapshot is modeled as

$$\mathbf{y}(t) = \mathbf{a}(\theta, \mathbf{p})s(t) + \mathbf{n}(t), \quad (3)$$

where  $s(t)$  is the transmitted source signal with average power  $P_s = \mathbb{E}[|s(t)|^2]$  and  $\mathbf{n}(t) \sim \mathcal{CN}(\mathbf{0}, \sigma_n^2 \mathbf{I}_M)$  represents the additive white Gaussian noise (AWGN) with zero mean and variance  $\sigma_n^2$ . The signal-to-noise ratio (SNR) at the transmitter side is defined as  $\text{SNR} \triangleq \frac{P_s}{\sigma_n^2}$ .

### C. Virtual Array Transformation

To align with [11], the second-order statistics of the received signal is exploited to expand the sensing aperture by virtual

array transformation from the covariance matrix. Define the snapshot matrix as  $\mathbf{Y} \triangleq [\mathbf{y}(1), \mathbf{y}(2), \dots, \mathbf{y}(T)] \in \mathbb{C}^{M \times T}$  and the corresponding covariance is given by  $\mathbf{R}_Y \triangleq \mathbb{E}[\mathbf{y}(t)\mathbf{y}(t)^H]$ . Consider the independence among AWGN and signal component, the covariance matrix  $\mathbf{R}_Y$  is approximated as

$$\mathbf{R}_Y \approx P_s \mathbf{a}(\theta, \mathbf{p}) \mathbf{a}(\theta, \mathbf{p})^H + \sigma_n^2 \mathbf{I}_M, \quad (4)$$

which can be readily extended into the case of multiple AoAs if the multi-path components are deemed as uncorrelated and the cross-terms equal to zeros in the covariance matrix [1]. Then vectorizing  $\mathbf{R}_Y$  yields the virtual received signal

$$\mathbf{y}_v = \text{vec}(\mathbf{R}_Y) \approx P_s (\mathbf{a}(\theta, \mathbf{p})^* \otimes \mathbf{a}(\theta, \mathbf{p})) + \sigma_n^2 \text{vec}(\mathbf{I}_M), \quad (5)$$

where the Kronecker term is known as the virtual difference co-array (DCA) and is determined by the set of position differences  $\{p_u - p_v\}$ . Conveniently, one could form a sensing AoA codebook by discretizing the angular domain into a grid  $\Theta = \{\vartheta_1, \dots, \vartheta_N\}$ . The sensing codebook  $\mathbf{A}(\mathbf{p}) \in \mathbb{C}^{M^2 \times N}$  is then constructed, whose  $n$ -th column is  $\mathbf{c}_n(\mathbf{p}) = \mathbf{a}(\vartheta_n, \mathbf{p})^* \otimes \mathbf{a}(\vartheta_n, \mathbf{p})$ , where the entry corresponding to the antenna pair  $(u, v)$  is  $[\mathbf{c}_n(\mathbf{p})]_{(v-1)M+u} = e^{-j2\pi(p_u - p_v) \cos \vartheta_n}$ .

### III. MINIMUM SPACING ANALYSIS

The minimum spacing in (1) is essential to FAA to prevent port overlap. However, the statistical behavior of port spacing under finite-aperture placement remains unclear. This section rigorously justifies the necessity of the minimum-spacing constraint  $d_{\min}$  by analyzing port spacing statistics under a random placement strategy. Specifically,  $M$  active ports are selected independently and uniformly at random within the fixed aperture  $[0, W_{\max}]$ . Let  $X_{(1)} < X_{(2)} < \dots < X_{(M)}$  denote the order statistics representing the sorted physical positions of active ports. The joint PDF is uniform over the correspondingly simplex  $\mathcal{D} = \{(x_1, \dots, x_M) \mid 0 \leq x_1 < \dots < x_M \leq W_{\max}\}$ , given by  $f(\mathbf{x}) = M!/W_{\max}^M$ . Let  $\Delta_{\min} = \min_{1 \leq i \leq M-1} \{X_{(i+1)} - X_{(i)}\}$  denote the minimum spacing random variable and we derive its PDF below.

**Proposition 1:** The expected minimum spacing for FAA should be set no smaller than

$$\mathbb{E}[\Delta_{\min}] = \int_0^{\frac{W_{\max}}{M-1}} \delta f_{\Delta_{\min}}(\delta) d\delta = \frac{W_{\max}}{M^2 - 1}, \quad (6)$$

where  $\delta \in [0, \frac{W_{\max}}{M-1}]$  and the PDF is given by

$$f_{\Delta_{\min}}(\delta) = \frac{M(M-1)}{W_{\max}} \left(1 - \frac{(M-1)\delta}{W_{\max}}\right)^{M-1}. \quad (7)$$

**Proof:** Initially, let the event  $\mathcal{E} = \{\Delta_{\min} > \delta\}$  imply that the spacing between every pair of adjacent ordered elements must exceed  $\delta$ , i.e.,  $X_{(i+1)} - X_{(i)} > \delta$  for all  $i = 1, \dots, M-1$ . Then, we derive the complementary cumulative distribution function (CCDF), denoted as  $\mathbb{P}(\Delta_{\min} > \delta)$ , in a *geometric model of probabilistic manner*. However, calculating the *volume* of this constrained high-dimensional region directly is intractable due to the coupled boundary conditions. To loosen the calculation demand, we introduce a new set of variables  $\mathbf{Y} = [Y_1, \dots, Y_M]^T$  defined as

$$Y_k = X_{(k)} - (k-1)\delta. \quad (8)$$

Therefore, the difference between adjacent  $Y_k$  is

$$\begin{aligned} Y_{i+1} - Y_i &= (X_{(i+1)} - i\delta) - (X_{(i)} - (i-1)\delta) \\ &= (X_{(i+1)} - X_{(i)}) - \delta. \end{aligned} \quad (9)$$

By (9), the original constraint  $X_{(i+1)} - X_{(i)} > \delta$  is equivalently converted to the standard ordering constraint  $Y_{i+1} > Y_i$ . Simultaneously, the original variable domain  $X_{(M)} \leq W_{\max}$  transforms to  $Y_M + (M-1)\delta \leq W_{\max} \rightarrow Y_M \leq W_{\max} - (M-1)\delta$ . Let  $W' = W_{\max} - (M-1)\delta$  denote the *effective aperture*.

The minimum-spacing constraint induces multiple exclusion zones in the joint domain, yielding a fragmented admissible region with coupled boundaries. The linear transformations in (8) and (9) remove these zones by index-dependent shifts of the ordered coordinates, mapping the region bijectively and volume-preservingly onto a contiguous standard simplex with reduced aperture. Thus, the feasible volume is obtained from the simplex  $\mathcal{S}' = \{(y_1, \dots, y_M) \mid 0 \leq y_1 < \dots < y_M \leq W'\}$ .

The Jacobian of this linear transformation is the determinant of a triangular matrix with ones on the diagonal, i.e.,  $|\det(\mathbf{J})| = 1$ . Therefore, the volume calculation preserves the differential relationship of  $d\mathbf{x} = d\mathbf{y}$ . The volume of the standard simplex  $\mathcal{S}'$  is simply  $(W')^M/M!$ . The probability is the ratio of the valid volume to the total volume  $(W_{\max}^M/M!)$

$$\begin{aligned} \mathbb{P}(\Delta_{\min} > \delta) &= \frac{\text{Vol}(\mathcal{S}')}{\text{Vol}(\mathcal{D})} \\ &= \frac{(W_{\max} - (M-1)\delta)^M}{W_{\max}^M} = \left(1 - \frac{(M-1)\delta}{W_{\max}}\right)^M. \end{aligned} \quad (10)$$

Differentiating  $F_{\Delta_{\min}}(\delta) = 1 - \mathbb{P}(\Delta_{\min} > \delta)$  with respect to  $\delta$  gives the PDF of  $\Delta_{\min}$  in (7), defined for the support  $\delta \in [0, \frac{W_{\max}}{M-1}]$ . The upper bound of the support, i.e.,  $\delta_{\max} = \frac{W_{\max}}{M-1}$ , corresponds to the ULA configuration. Since the ULA maximizes the minimum spacing by distributing elements evenly, no randomized placement can achieve a minimum spacing larger than this value. ■

**Remark 1:** This result reveals a fundamental limitation of random FAA. While the element spacing in a ULA decreases linearly with  $M$ , i.e.,  $\propto M^{-1}$ , the expected minimum spacing in a random FAA decays quadratically, i.e.,  $\propto M^{-2}$ .

### IV. UNIVERSAL CRB FOR FINITE-APERTURE ARRAY

In this section, we derive the exact closed-form expression for the CRB under finite-aperture budget. By explicitly relating the CRB to the antenna position variance, we provide a theoretical benchmark universally applicable for different systems and different antenna placement. Recalling the received signal in (3), to generalize the CRB to different carrier frequency, we rewrite the steering vector  $\mathbf{a}(\theta, \mathbf{p})$  in (2) as

$$\mathbf{a}(\theta, \mathbf{p}) = \left[ e^{-jkp_1 \cos(\theta)}, \dots, e^{-jkp_M \cos(\theta)} \right]^T, \quad (11)$$

where  $k = 2\pi/\lambda$  is the wavenumber. If the antenna positions are normalized by  $\lambda$ , i.e.,  $p_m \leftarrow p_m/\lambda$ , then the steering component becomes  $e^{-j2\pi p_m \cos \theta}$ , equivalent to setting  $\lambda = 1$ . In the sequel, we will omit the variable term  $\mathbf{p}$  and treat it as deterministic constants to derive CRB for angle  $\theta$ .

Under the deterministic signal model, the Fisher Information Matrix (FIM) element  $J_{\theta\theta}$  with respect to the angle  $\theta$  is given by the Slepian-Bangs formula [13, Section 3.3]

$$J_{\theta\theta} = \frac{2TP_s}{\sigma_n^2} \operatorname{Re} \{ \dot{\mathbf{a}}^H(\theta) \mathbf{P}_{\mathbf{a}}^\perp \dot{\mathbf{a}}(\theta) \}, \quad (12)$$

where  $\operatorname{Re}\{\cdot\}$  takes the real part of the variable,  $P_s$  is the signal power,  $\dot{\mathbf{a}}(\theta)$  denotes the partial derivative  $\frac{\partial \mathbf{a}(\theta)}{\partial \theta}$ , and  $\mathbf{P}_{\mathbf{a}}^\perp$  is the orthogonal projection matrix onto the null space of  $\mathbf{a}(\theta)$ :

$$\mathbf{P}_{\mathbf{a}}^\perp = \mathbf{I}_M - \frac{\mathbf{a}(\theta)\mathbf{a}^H(\theta)}{\mathbf{a}^H(\theta)\mathbf{a}(\theta)} = \mathbf{I}_M - \frac{1}{M} \mathbf{a}(\theta)\mathbf{a}^H(\theta), \quad (13)$$

where the simplification considers  $|\mathbf{a}|_m = 1$  and  $\mathbf{a}^H\mathbf{a} = M$ . Next, we explain how to derive the CRB step-by-step below.

### A. Derivative of the Steering Vector

To obtain an explicit relationship between estimation accuracy and array geometry (port placement  $\mathbf{p}$ ), the quadratic term in (12). Since the  $m$ -th element of the steering vector is  $[\mathbf{a}(\theta)]_m = e^{-j k p_m \cos(\theta)}$ , its derivative with respect to  $\theta$  is

$$\begin{aligned} \frac{\partial [\mathbf{a}]_m}{\partial \theta} &= \frac{\partial}{\partial \theta} \left( e^{-j k p_m \cos(\theta)} \right) \\ &= e^{-j k p_m \cos(\theta)} \cdot (-j k p_m) \cdot (-\sin(\theta)) = j k p_m \sin(\theta) [\mathbf{a}]_m, \end{aligned} \quad (14)$$

which can be written in a more compact form  $\dot{\mathbf{a}}(\theta) = j k \sin(\theta) \mathbf{D} \mathbf{a}(\theta)$ , where  $\mathbf{D} = \operatorname{diag}(p_1, p_2, \dots, p_M)$  is a diagonal matrix containing the antenna positions.

### B. Expansion of the Quadratic Form

Plugging (14) into the quadratic term  $\mathcal{Q} = \dot{\mathbf{a}}^H \mathbf{P}_{\mathbf{a}}^\perp \dot{\mathbf{a}}$  in (12)

$$\mathcal{Q} = \dot{\mathbf{a}}^H \left( \mathbf{I}_M - \frac{1}{M} \mathbf{a} \mathbf{a}^H \right) \dot{\mathbf{a}} = \underbrace{\dot{\mathbf{a}}^H \dot{\mathbf{a}}}_{\text{Term I}} - \frac{1}{M} \underbrace{\dot{\mathbf{a}}^H \mathbf{a} \mathbf{a}^H \dot{\mathbf{a}}}_{\text{Term II}}, \quad (15)$$

where *Term I* and *Term II* can be further simplified. For *Term I*, plugging (14) and recalling that  $|\mathbf{a}|_m = 1$ , the squared norm of the derivative vector can be written as

$$\dot{\mathbf{a}}^H \dot{\mathbf{a}} = \sum_{m=1}^M |j k p_m \sin(\theta) [\mathbf{a}]_m|^2 = k^2 \sin^2(\theta) \sum_{m=1}^M p_m^2. \quad (16)$$

Then for *Term II*, we first evaluate the inner product

$$\begin{aligned} \mathbf{a}^H \dot{\mathbf{a}} &= \sum_{m=1}^M [\mathbf{a}]_m^* \cdot (j k p_m \sin(\theta) [\mathbf{a}]_m) \\ &= j k \sin(\theta) \sum_{m=1}^M \underbrace{[\mathbf{a}]_m^* [\mathbf{a}]_m}_{=1} p_m = j k \sin(\theta) \sum_{m=1}^M p_m. \end{aligned} \quad (17)$$

Consequently, *Term II* becomes

$$\dot{\mathbf{a}}^H \mathbf{a} \mathbf{a}^H \dot{\mathbf{a}} = |\dot{\mathbf{a}}^H \dot{\mathbf{a}}|^2 = k^2 \sin^2(\theta) \left( \sum_{m=1}^M p_m \right)^2. \quad (18)$$

Substituting (17) and (18) back into (15) yields

$$\mathcal{Q} = k^2 \sin^2(\theta) \left[ \sum_{m=1}^M p_m^2 - \frac{1}{M} \left( \sum_{m=1}^M p_m \right)^2 \right]. \quad (19)$$

Let  $\bar{p} = \frac{1}{M} \sum_{m=1}^M p_m$  denote the geometric centroid of the array. Utilizing the variance identity  $\sum(x_i - \bar{x})^2 = \sum x_i^2 -$

$\frac{1}{M}(\sum x_i)^2$ , the term in the brackets of (19) is exactly the *effective aperture variance*, denoted as

$$\sum_{m=1}^M p_m^2 - \frac{1}{M} \left( \sum_{m=1}^M p_m \right)^2 = \sum_{m=1}^M (p_m - \bar{p})^2 \triangleq \mathcal{L}_{\text{geo}}(\mathbf{p}). \quad (20)$$

From (19), we have the closed-form quadratic term

$$\mathcal{Q} \triangleq \dot{\mathbf{a}}^H(\theta) \mathbf{P}_{\mathbf{a}}^\perp \dot{\mathbf{a}}(\theta) = k^2 \sin^2(\theta) \mathcal{L}_{\text{geo}}(\mathbf{p}), \quad (21)$$

where  $\mathcal{L}_{\text{geo}}(\mathbf{p}) \triangleq \sum_{m=1}^M (p_m - \bar{p})^2$ ,  $\bar{p} = \frac{1}{M} \sum_{m=1}^M p_m$ . Noting that  $\mathcal{Q}$  is real and non-negative, we hence have  $\operatorname{Re}\{\mathcal{Q}\} = \mathcal{Q}$ . Substituting (21) into (12), we obtain

$$\begin{aligned} J_{\theta\theta} &= \frac{2TP_s}{\sigma_n^2} \operatorname{Re} \{ \dot{\mathbf{a}}^H(\theta) \mathbf{P}_{\mathbf{a}}^\perp \dot{\mathbf{a}}(\theta) \} = \frac{2TP_s}{\sigma_n^2} \mathcal{Q} \\ &= \frac{2TP_s}{\sigma_n^2} k^2 \sin^2(\theta) \mathcal{L}_{\text{geo}}(\mathbf{p}). \end{aligned} \quad (22)$$

Using the SNR definition, (22) becomes  $J_{\theta\theta} = 2T \cdot \text{SNR} \cdot k^2 \sin^2(\theta) \mathcal{L}_{\text{geo}}(\mathbf{p})$ . Finally, we derive the universal closed-form CRB via the inverse of the FIM element [14, Chapter 3]

$$\text{CRB}(\theta) = (J_{\theta\theta})^{-1} = \frac{1}{2T \cdot \text{SNR} \cdot k^2 \sin^2(\theta) \mathcal{L}_{\text{geo}}(\mathbf{p})}. \quad (23)$$

**Remark 2:** If we use the physical wavenumber  $k = 2\pi/\lambda$ ,

$$\begin{aligned} \text{CRB}(\theta) &= \frac{1}{2T \cdot \text{SNR} \cdot \left( \frac{4\pi^2}{\lambda^2} \right) \sin^2(\theta) \mathcal{L}_{\text{geo}}(\mathbf{p})} \\ &= \frac{\lambda^2}{8\pi^2 T \cdot \text{SNR} \cdot \sin^2(\theta) \mathcal{L}_{\text{geo}}(\mathbf{p})}. \end{aligned} \quad (24)$$

For the wavelength-normalized case in (2), the factor  $\lambda^2$  in (24) is absorbed into  $\mathcal{L}_{\text{geo}}(\mathbf{p})$ , and the CRB can be written as  $\text{CRB}(\theta) = \frac{1}{8\pi^2 T \cdot \text{SNR} \cdot \sin^2(\theta) \cdot \mathcal{L}_{\text{geo}}(\mathbf{p})}$  with  $\lambda = 1$ .

**Remark 3:** The expression in (24) reveals a trade-off between **estimation precision** and **ambiguity suppression**. Maximizing the geometric variance  $\mathcal{L}_{\text{geo}}$  by placing elements near the boundaries ( $p_m \rightarrow 0$  or  $W_{\max}$ ) minimizes the CRB and achieves the highest precision, but induces **false spectral peaks** and **severe beam misdirection**. In contrast, uniform spacing suppresses these **false peaks** at the cost of a **smaller effective aperture**, resulting in lower precision.

## V. ARRAY PLACEMENT ALGORITHM DESIGN

Remark 3 has thoroughly explained the trade-off between the main-lobe (estimation precision) and the side-lobe (ambiguity suppression) under finite-aperture budget. Another problem is how to conduct practical design under the observations in (23). This section provides an example for practical design starting from the following remark.

**Remark 4:** In [11, (35)], an AoA mean-squared error (AoAMSE) upperbound is predicted as

$$\text{AoAMSE} = \mathbb{E} \left\{ \left| \cos \theta_i - \cos \hat{\theta}_i \right|^2 \right\} \leq \frac{16\sigma_z^4 \gamma_{\max}(\mathbf{p})}{\bar{\lambda}^2(\mathbf{p}) M^4}, \quad (25)$$

where  $\sigma_z^2$  denotes the variance of the interference-plus-noise component,  $\gamma_{\max}(\mathbf{p})$  is the largest eigenvalue of  $\mathbf{A}^H(\mathbf{p}) \mathbf{A}(\mathbf{p})$  where  $\mathbf{A}(\mathbf{p})$  is the AoA sensing matrix determined by port placement and  $\bar{\lambda}^2(\mathbf{p}) = \frac{1}{M^2} \sum_{u,v} (p_u - p_v)^2$ .

Remark 4 encourages us to formulate the antenna placement into an optimization problem of  $\arg \min_{\mathbf{p}} \gamma_{\max}(\mathbf{p}) / \bar{\lambda}^2(\mathbf{p})$ .

With logarithm-conversion, we get the AoAMSE minimization optimization expression as

$$\arg \min_{\mathbf{p}} J(\mathbf{p}) = \ln(\gamma_{\max}(\mathbf{p})) - \ln(\bar{\lambda}^2(\mathbf{p})), \quad (26)$$

where if the Lagrange's identity is applied, we observe that the term  $\bar{\lambda}^2(\mathbf{p}) = \frac{1}{M^2} \sum_{u,v} (p_u - p_v)^2$  is directly proportional to the geometric variance, i.e.,  $\sum_{u=1}^M \sum_{v=1}^M (p_u - p_v)^2 = 2M \sum_{m=1}^M (p_m - \bar{p})^2 = 2M \mathcal{L}_{\text{geo}}(\mathbf{p})$ . Thus, minimizing  $-\ln(\bar{\lambda}^2)$  becomes equivalent to minimizing the CRB, while minimizing  $\ln(\gamma_{\max})$  suppresses sidelobes. Expression (26) thereby seeks the Pareto-optimal configuration between *estimation precision* and *ambiguity resolution*. In the sequel, we propose a gradient-based algorithm to solve (26).

### A. Gradient Target Function Formulation

Here, we first clarify the Gram matrix and its dominant eigenvalue as  $\mathbf{Q}(\mathbf{p}) \triangleq \mathbf{A}(\mathbf{p})^H \mathbf{A}(\mathbf{p})$ ,  $\gamma_{\max}(\mathbf{p}) \triangleq \lambda_{\max}(\mathbf{Q}(\mathbf{p}))$  and specify the effective squared aperture term as  $\bar{\lambda}^2(\mathbf{p}) \triangleq \frac{1}{M^2} \sum_{u=1}^M \sum_{v=1}^M (2\pi(p_u - p_v))^2$ . Based on (26), the following target function is formulated as

$$\min_{\mathbf{p}} \ln(\lambda_{\max}(\mathbf{A}(\mathbf{p})^H \mathbf{A}(\mathbf{p}))) - \ln\left(\frac{1}{M^2} \sum_{u,v} (2\pi(p_u - p_v))^2\right) \quad (27a)$$

$$\text{s.t. } p_1 = 0, p_M = W_{\max}, p_m - p_{m-1} \geq d_{\min}. \quad (27b)$$

### B. Gradient Update Derivation

To apply gradient descent, we derive the gradient of  $J(\mathbf{p})$  with respect to the  $m$ -th position  $p_m$ ,  $m = 2, \dots, M-1$ , which consists of two terms

$$\frac{\partial J}{\partial p_m} = \frac{1}{\gamma_{\max}} \frac{\partial \gamma_{\max}}{\partial p_m} - \frac{1}{\bar{\lambda}^2} \frac{\partial \bar{\lambda}^2}{\partial p_m}, \quad (28)$$

where the two-derivative terms are:

$$\frac{\partial \gamma_{\max}}{\partial p_m} = \mathbf{u}_{\max}^H \frac{\partial \mathbf{Q}}{\partial p_m} \mathbf{u}_{\max}, \quad \frac{\partial \bar{\lambda}^2}{\partial p_m} = \frac{16\pi^2}{M^2} \sum_{k=1}^M (p_m - p_k), \quad (29)$$

where  $\mathbf{u}_{\max}$  is the unit-norm eigenvector of  $\mathbf{Q}$  associated with  $\gamma_{\max}$ . In (28), the term  $-\frac{\partial \bar{\lambda}^2}{\partial p_m}$  acts like pushing the antenna elements away from the array's centroid to maximize spatial spread, while  $\frac{\partial \gamma_{\max}}{\partial p_m}$  adjusts positions to minimize correlation.

### C. Algorithm Design

To solve (27), a projected gradient descent (PGD) algorithm is proposed in Algorithm 1. The key modification is that we only update  $p_2, \dots, p_{M-1}$ . The *projection* step is conducted by a feasibility restoration mapping: sorting, edge pinning, and enforcing minimum spacing through forward/backward corrections, where  $\beta$  and  $\alpha$  are the momentum coefficient and gradient coefficient respectively. Notably, gradient-method is initialization-sensitive but guarantees to a local minimum value [15, Section 2.3]. We initialize the placement vector  $\mathbf{p}$  by [3, Table II] or [11, Table II] for good performance.

### Algorithm 1: Joint Continuous Port Optimization

---

**Input:**  $M$ , Aperture  $W_{\max}$ , Angle Grid  $\Theta$ , Step  $\alpha$ , Min spacing  $d_{\min}$ .  
**Output:** Optimized positions  $\mathbf{p}^*$ .

1 **Initialization:** Get discrete MRA indices  $\mathcal{I}_{\text{MRA}}$  [3, Table II] or [11, Table II];  
2 Scale indices:  $\mathbf{p}^{(0)} = \frac{\mathcal{I}_{\text{MRA}}}{\max(\mathcal{I}_{\text{MRA}})} \times W_{\max}$ ;  
3 **for**  $t = 0$  **to**  $T_{\max}$  **do**  
4   Compute  $\gamma_{\max}$  and  $\bar{\lambda}^2$ ;  
5   Compute  $\nabla \gamma_{\max}$  and  $\nabla \bar{\lambda}^2$  via (29);  
6   Combine gradients:  $\nabla J = \frac{\nabla \gamma_{\max}}{\gamma_{\max}} - \frac{\nabla \bar{\lambda}^2}{\bar{\lambda}^2}$ ;  
7   **Update:**  $\hat{p}_m = \beta p_m^{(t)} - \alpha \nabla J_m$ ;  
8   **Projection:**  
9     1. Sort  $\tilde{\mathbf{p}}$ ;  
10     2. Pin Edges: Set  $\tilde{p}_1 = 0, \tilde{p}_M = W_{\max}$ ;  
11     3. Enforce  $p_m - p_{m-1} \geq d_{\min}$  (e.g., forward/backward corrections);  
12     **if** *Converged* **then**  
13       | Break;  
14     **end**  
15 **end**

---

### D. Computational Complexity

The computational cost is dominated by the construction and eigen-decomposition of the Gram matrix  $\mathbf{Q} \in \mathbb{C}^{N \times N}$ . Specifically, the per-iteration complexity scales as  $\mathcal{O}(N^3 + M^2 N^2)$ , where  $\mathcal{O}(N^3)$  accounts for the eigenvalue evaluation and  $\mathcal{O}(M^2 N^2)$  for the matrix construction and gradient updates.

## VI. NUMERICAL RESULTS

Here, we evaluate our analytical results and algorithm design. The common setups are as follows. All antenna positions are normalized by the wavelength ( $\lambda = 1$ ), and the aperture length is set to  $W_{\max} = (M-1) \times \frac{1}{2}$ , corresponding to a half-wavelength ULA. For codebook construction and evaluations of all  $\gamma_{\max}$  and  $\bar{\lambda}^2$ , we adopt a uniform grid  $\Theta$  with  $\theta \in [0, \pi]$  with  $N = 180$  grid points. Different schemes are compared, and their antenna placement methods are summarized as follows:

- *ULA*:  $p_m = (m-1) \times \frac{1}{2}$ .
- *Discrete FAS (Scaled MRA)*: the MRA indices are linearly scaled into  $[0, W_{\max}]$  via  $p = \frac{\mathcal{I}}{\max(\mathcal{I})} W_{\max}$ .
- *Continuous FAS*: initialized by the scaled MRA positions and optimized using Algorithm 1.

The antenna placement set of *Discrete FAS* is initialized following [11, Table II]. The minimum spacing is chosen according to the random-FAS expectation derived in Section III, i.e.,  $d_{\min} = \frac{W_{\max}}{M^2 - 1}$ . For Algorithm 1, we set  $\alpha = 5 \times 10^{-4}$ ,  $\beta = 0.9$ , and  $T_{\max} = 1000$ . All sensing codebooks are constructed from the covariance matrix.

The results in Fig. 1 explicitly show the agreement between Monte Carlo samples and the predicted distributions, validating the fundamental limits of the minimum port placement constraint in Proposition 1.

In Fig. 2, we see that the proposed gradient-based algorithm converges under various settings, and the optimized objective value is significantly lower than that of the conventional ULA. The small step size  $\alpha = 5 \times 10^{-4}$  explains the requirement of several hundred iterations for convergence. Nevertheless, the

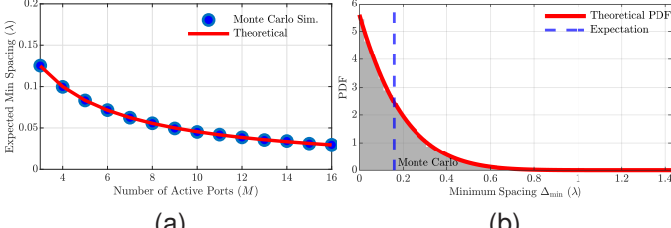


Fig. 1: Empirical and theoretical  $E[\Delta_{\min}]$  of the minimum placement constraint  $d_{\min}$ : (a)  $M \in \{3, 4, \dots, 16\}$ ,  $W_{\max} = (M - 1) \times 0.5$ ; (b)  $M = 8$ ,  $W = 10$ .

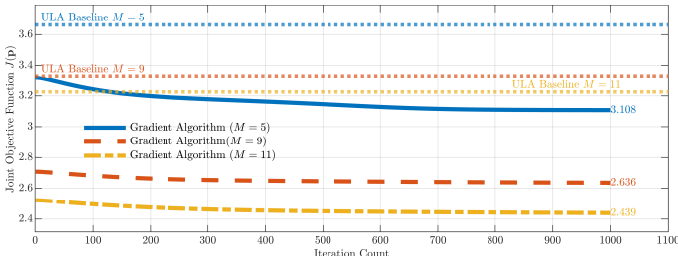


Fig. 2: Convergence behavior of Algorithm 1 under  $M \in \{5, 9, 11\}$ .

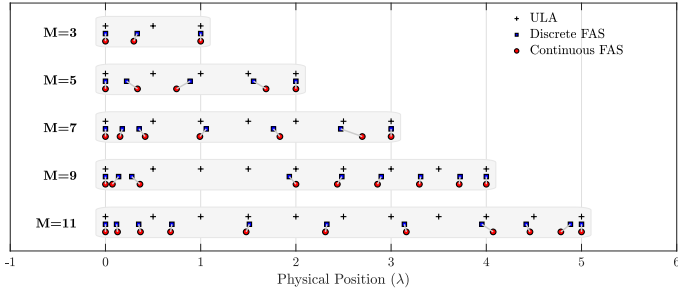


Fig. 3: Illustration of different arrays for  $M \in \{3, 5, 7, 9, 11\}$ .

array design is performed offline and requires only a one-time computation. Different antenna placements are also illustrated in Fig. 3 for clarity.

Compared with the ULA, Fig. 4 indicates that FAA exhibits a much improved sensing matrix structure with a significantly reduced maximum eigenvalue. In terms of CRB, a reduction of about 30% is observed at  $M = 11$ . The continuous and discrete cases yield similar CRB performance, and the performance gap between FAA and ULA widens as  $M$  increases.

Finally, Fig. 5 illustrates that with increasing aperture size, the AoAMSE gap between FAS and FAA becomes more pronounced. For  $M = 5$ , an average AoAMSE reduction of 42.5% is achieved across different SNR regimes.

## VII. CONCLUSION

In this letter, we characterized the expected minimum placement gap for FAA via an accurate closed-form PDF derivation. A closed-form CRB applicable to general finite-aperture array designs was further derived. Beyond the theoretical analysis, we devised a practical array optimization algorithm that substantially reduces both the CRB and the AoAMSE under a fixed aperture. Numerical results confirmed the superiority of fluid antennas over conventional ULAs for finite-aperture array design. How to realize practical design algorithm with loose initialization would be a crucial future direction.

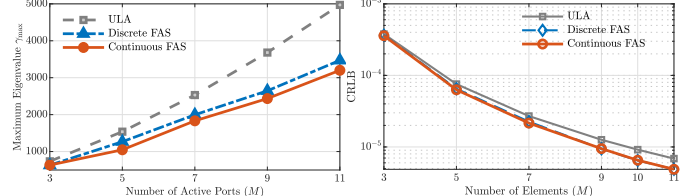


Fig. 4: Maximum eigenvalue of the sensing codebook  $\mathbf{A}$  and CRB of different arrays: (a)  $M \in \{3, 5, 7, 9, 11\}$ ; (b) SNR = 10 dB, target angle  $\theta = 15^\circ$ , snapshots  $T = 100$ .

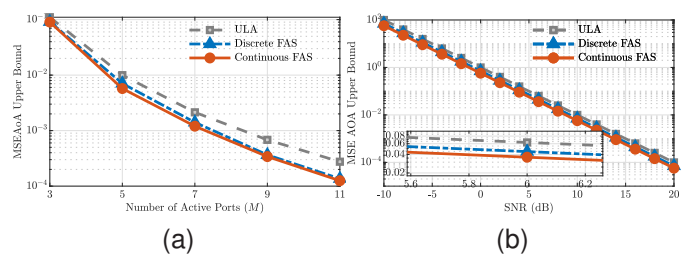


Fig. 5: AoAMSE upper bound of different arrays: (a) SNR = 10 dB,  $M \in \{3, 5, 7, 9, 11\}$ ; (b) SNR ∈ {−10, −8, ..., 20} dB,  $M = 5$ .

## REFERENCES

- [1] H. L. Van Trees, *Optimum Array Processing: Part IV of Detection, Estimation, and Modulation Theory*. New York, NY, USA: Wiley-Interscience, 2002.
- [2] C.-L. Liu and P. P. Vaidyanathan, “Cramér–Rao bounds for coprime and other sparse arrays, which find more sources than sensors,” *Digit. Signal Process.*, vol. 61, pp. 43–61, Feb. 2017.
- [3] A. T. Moffet, “Minimum-redundancy linear arrays,” *IEEE Trans. Antennas Propag.*, vol. 16, no. 2, pp. 172–175, Mar. 1968.
- [4] K. K. Wong, *et al.*, “Fluid antenna systems,” *IEEE Trans. Wireless Commun.*, vol. 20, no. 3, pp. 1950–1962, Mar. 2021.
- [5] W. K. New, *et al.*, “A tutorial on fluid antenna system for 6G networks: Encompassing communication theory, optimization methods and hardware designs,” *IEEE Commun. Surv. Tuts.*, vol. 27, no. 4, pp. 2325–2377, Aug. 2025.
- [6] H. Hong, *et al.*, “A contemporary survey on fluid antenna systems: Fundamentals and networking perspectives,” *IEEE Trans. Netw. Sci. Eng.*, vol. 13, pp. 2305–2328, 2026.
- [7] W. K. New, *et al.*, “Fluid antenna systems: Redefining reconfigurable wireless communications,” *IEEE J. Sel. Areas Commun.*, DOI:10.1109/JSAC.2025.3632097, 2026.
- [8] T. Wu, *et al.*, “Fluid antenna systems enabling 6G: Principles, applications, and research directions,” to appear in *IEEE Wireless Commun.*, DOI:10.1109/MWC.2025.3629597, 2025.
- [9] J. Xu, *et al.*, “Fluid antenna-enhanced flexible beamforming,” *arXiv preprint*, arXiv:2511.22163, 2025.
- [10] B. Tang, *et al.*, “Full-duplex FAS-assisted base station for ISAC,” *IEEE Trans. Wireless Commun.*, vol. 25, pp. 2922–2938, 2025.
- [11] Z. Zhang, *et al.*, “On fundamental limits for fluid antenna-assisted integrated sensing and communications for unsourced random access,” *IEEE J. Sel. Areas Commun.*, DOI:10.1109/JSAC.2025.3608113, 2025.
- [12] Z. Zhang, *et al.*, “On fundamental limits of slow-fluid antenna multiple access for unsourced random access,” *IEEE Wireless Commun. Lett.*, vol. 14, no. 11, pp. 3455–3459, Nov. 2025.
- [13] P. Stoica and R. Moses, *Spectral Analysis of Signals*. Upper Saddle River, NJ, USA: Prentice Hall, 2005.
- [14] S. M. Kay, *Fundamentals of Statistical Signal Processing, Vol. I: Estimation Theory*. Englewood Cliffs, NJ, USA: Prentice Hall, 1993.
- [15] D. P. Bertsekas, *Nonlinear Programming*, 2nd ed. Belmont, MA, USA: Athena Scientific, 1999.